International Journal of Modern Physics B
Vol. 23, Nos. 6 & 7 (2009) 1217–1222
© World Scientific Publishing Company

World Scientific
www.worldscientific.com

CHARACTERIZATION OF SHEAR BANDS IN TWO BULK METALLIC GLASSES WITH DIFFERENT INHERENT PLASTICITY

JIANSHENG GU

National Microgravity Laboratory, Institute of Mechanics,
Chinese Academy of Sciences, Beijing 100190, China

LEI LI[*], TAIHUA ZHANG[†], PENG JIANG[†], BINGCHEN WEI[*,‡] and ZHIWEI SUN[*]

[*]*National Microgravity Laboratory, Institute of Mechanics,*
Chinese Academy of Sciences, Beijing 100190, China
[†]*State Key Laboratory of Nonlinear Mechanics, Institute of Mechanics,*
Chinese Academy of Sciences, Beijing 100190, China
[‡]*weibc@imech.ac.cn*

Shear banding characterization of $Zr_{64.13}Cu_{15.75}Ni_{10.12}Al_{10}$ and $Zr_{65}Cu_{15}Ni_{10}Al_{10}$ bulk metallic glasses (BMGs) with significant difference in inherent plasticity and quite similar chemical composition was studied by depth sensitive macroindentaion tests with conical indenter. Well-developed shear band pattern can be found for both BMGs after indentation. Distinct difference in the shear band spacing, scale of plastic deformation region and the shear band branching in the two BMGs account for the different plasticity.

Keywords: Bulk metallic glass; plastic deformation; shear band; depth sensitive indentation.

1. Introduction

Bulk metallic glass (BMG) materials possess remarkable physical, chemical, and mechanical properties and have potential applications in many areas, which have created extensive interest among scientists and engineers[1-3]. However, below the glass-transition temperature, plastic deformation of metallic glasses is localized into narrow shear bands, followed by the rapid propagation of these shear bands and sudden fracture[3,4]. Although most BMGs appear to be inherently brittle at ambient temperature, some impressive improvements in plasticity (for example, > 100% plastic strain under compression) have been reported[5-10]. Apparently, the improvement the ductility of metallic glasses can be obtained through promoting the initiation of a larger number of shear bands and inhibiting shear band propagation. Profuse shear bands can be found near the fracture surface of the ductile BMGs[5-10]. However, the larger number of shear bands is correlated to their large underwent total plastic strain. The direct comparison of shear bands feature of BMGs with significant difference in inherent ductility and at the same plastic strain without failure should be helpful to further understanding the operation of shear band and their correlation with the ductility of metallic glasses. Indentation test is a useful way for this study, as significant plastic strain can be achieved even for the brittle BMGs and the

control of the equivalent plastic strain is convenient. Deformation feature of BMGs around the indents has been investigated through a variety of indenters: pyramidal, spherical and conical[11-14]. Here we used a depth sensitive macroindentation technique with conical indenter to characterize the shear band feature of two typical BMGs with large difference in inherent ductility and quite similar chemical composition ($Zr_{64.13}Cu_{15.75}Ni_{10.12}Al_{10}$[5] and $Zr_{65}Cu_{15}Ni_{10}Al_{10}$ BMG[15]).

2. Experiment Procedure

The two master alloys with the composition of $Zr_{65}Cu_{15}Ni_{10}Al_{10}$, $Zr_{64.13}Cu_{15.75}Ni_{10.12}Al_{10}$ were prepared by arc melting the pure elements in a titanium-gettered argon atmosphere. Cylindrical rods with 3 mm diameter were produced by chill-casting into a copper mould. The structure of the as-cast samples was characterized by X-ray diffraction (XRD) in a Philips PW 1050 diffractometer using Cu K_α radiation. Thermal analysis was performed with a Netzsch 404C differential scanning calorimeter (DSC) at a heating rate of 0.33 K/s under argon atmosphere. The uniaxial compressive tests on cylindrical samples of 3 mm in diameter and 6 mm in length were performed in a commercial MTS testing machine at room temperature. The crosshead was moved at a constant speed with an initial strain rate of $1.0\times10^{-4}s^{-1}$.

The samples for indentation tests were cut from the same rod for compression test and at the position very closed to that of the compression specimen. The indentation specimens were polished by successive polishing steps to 1 μm finish using diamond pastes. Depth sensitive indentation experiments were conducted using a conical indenter (semiangle, β=60°). The indentation measurements were performed in a displacement-control mode to a load limit of 400N with the constant displacement rate 0.5 μm/s. Optical microscope and scanning electron microscopy (SEM) were used to study the surface morphology around the indents.

3. Results and Discussion

Figure 1 shows the DSC results of the as-cast $Zr_{64.13}Cu_{15.75}Ni_{10.12}Al_{10}$ and $Zr_{65}Cu_{15}Ni_{10}Al_{10}$ rods with 3 mm diameter at the heating rate of 0.33 K/s. Both alloys show an endothermic reaction caused by glass transition, followed by a sharp exothermic reaction caused by crystallization. The onset temperature of glass transition (T_g) and the crystallization temperature (T_x) are listed in Table 1. These values agree well with the reported results of the BMGs with the same chemical composition[5,15]. XRD patterns of the two alloys are presented in the inset of Fig. 1, which exhibits a diffuse halo and further confirms the amorphous structure of the specimens.

Quasi-static uniaxial compressive tests for the two BMGs were performed on the samples with 3 mm diameter and 6 mm length at an initial strain rate of $1.0\times10^{-4}s^{-1}$. The true stress-strain curves are shown in Fig 2. The elastic modulus (E) and the yield strength ($\sigma_{0.2}$) are 77.2 GPa and 1708 MPa respectively for $Zr_{64.13}Cu_{15.75}Ni_{10.12}Al_{10}$ BMG, and are 77.21 GPa and 1661 MPa respectively for the $Zr_{65}Cu_{15}Ni_{10}Al_{10}$ BMG. These

values are in agreement with reported results[5,16]. $Zr_{65}Cu_{15}Ni_{10}Al_{10}$ BMG exhibits an elastic limit of 2.27% and plastic strain of about 1.0%. $Zr_{64.13}Cu_{15.75}Ni_{10.12}Al_{10}$ BMG exhibits an elastic limit of 2.34% and a large compressive plastic strain of about 13.22%. Although this plasticity is lower than reported result[5] (where the compression specimen is 2mm in diameter), the alloy does show significant plasticity with respect to the brittleness of the $Zr_{65}Cu_{15}Ni_{10}Al_{10}$ BMG. These mechanical properties, as well as Poisson's ratio (ν) taken from Ref. [5,16] of the two BMGs are also listed in Table 1.

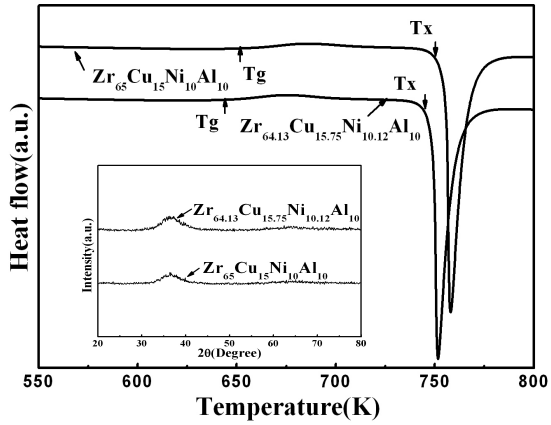

Fig. 1. DSC curves of the two BMGs at the heating rate of 0.33 K/s. Inset is XRD patterns of the two BMGs.

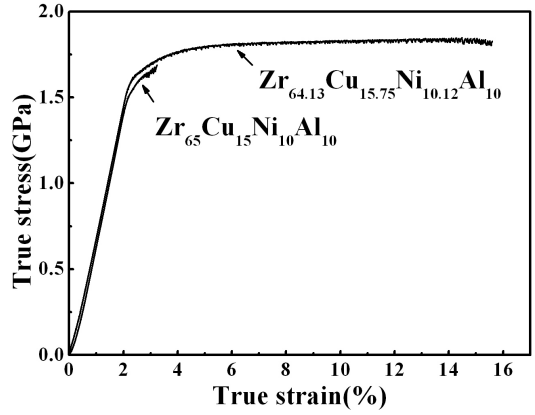

Fig. 2. True stress-strain curves of the two BMGs during compression at the initial strain rate of $1.0\times10^{-4}s^{-1}$.

Table 1. The thermal and mechanical properties of the two BMGs.

Alloy	T_g (K)	T_x (K)	ν	E (GPa)	$\sigma_{0.2}$ (MPa)
$Zr_{64.13}Cu_{15.75}Ni_{10.12}Al_{10}$	643	745	0.377	77.20	1708
$Zr_{65}Cu_{15}Ni_{10}Al_{10}$	652	750	0.355	77.21	1661

To clarify the shear band features in the two BMGs with similar chemical composition but with significant difference in compressive plasticity, depth sensitive macroindentation tests were used to characterize the plastic deformation region feature of the two BMGs, due to their superiority of the observation of the mechanisms of plastic deformation under well-controlled condition[11-14]. Here, macroindentation tests were conducted using a conical indenter to a load limit of about 400 N at a constant displacement rate of 0.5 μm/s. The diameter of the indents after indentation tests is almost same for the two BMGs of about 320 μm. This indicates that the plastic deformation stain of the two BMG is similar after the indentation tests.

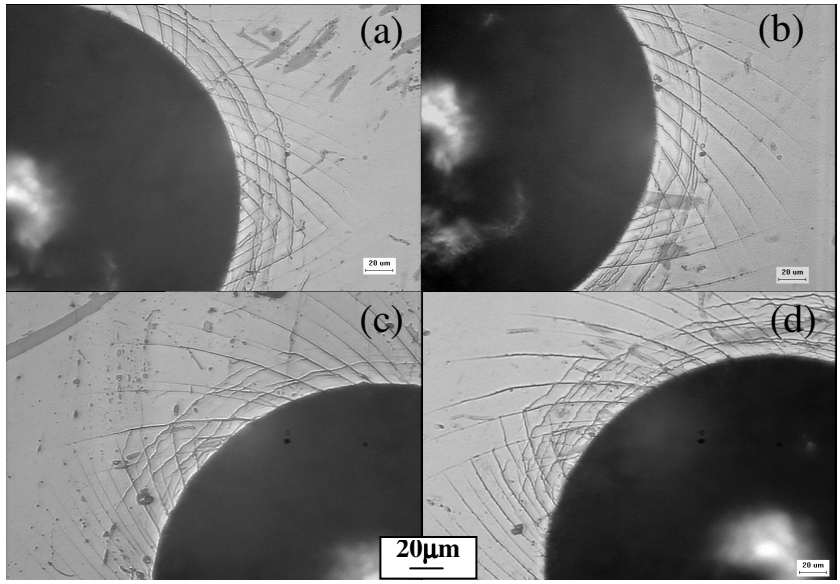

Fig. 3. Optical micrographs of indents after indentation tests at the maximum load of 400N with the constant displacement rate of 0.5μm/s. (a)(c) $Zr_{64.13}Cu_{15.75}Ni_{10.12}Al_{10}$ BMG, (b)(d)$Zr_{65}Cu_{15}Ni_{10}Al_{10}$ BMG.

The surface morphologies of indents after indentation tests for the two BMGs are shown in Fig 3. Two different kinds of shear bands are noticeable in both alloys: radial shear bands and concentric shear bands. The former type consists of two sets of shear bands (nearly mutually orthogonal), originating at the edge of the indent and following an outward logarithmic spiral pattern with remarkable shear band spacing. The latter type is circular shear band around the indent, again spreading away from the print but with smaller shear band spacing. It could be found in Fig. 3 that the two BMGs show quite similar shear band pattern. However, Careful examination of the shear band features indicates that the number density of radial shear bands in the $Zr_{64.13}Cu_{15.75}Ni_{10.12}Al_{10}$ BMG is definitely larger than that in the $Zr_{65}Cu_{15}Ni_{10}Al_{10}$ BMG, whereas no distinct difference is found for feature of the circular shear bands. The average shear band spacing for the radial shear bands at the edge of the indent of the former BMG is about

13 μm, while the value is about 17 μm for the latter BMG (Figs. 3 a, b). This means the radial shear band spacing in $Zr_{64.13}Cu_{15.75}Ni_{10.12}Al_{10}$ BMG with significant macro-scaled plasticity is about 23% less than that in the brittle $Zr_{65}Cu_{15}Ni_{10}Al_{10}$ BMG. As the two BMGs undergo nearly equivalent total plastic strain under the same indentation test condition, the smaller spacing and larger number density of radial shear bands in the $Zr_{64.13}Cu_{15.75}Ni_{10.12}Al_{10}$ BMG suggest that each single shear band carried much less shear strain during the plastic deformation of the specimen. It is assumed that fracture in metallic glasses initiates when the shear displacement on a particular shear band reaches a critical value, while the strain on any other shear band is still relatively small[3,17]. The relative homogeneous and fine shear band pattern formed during plastic deformation in the $Zr_{64.13}Cu_{15.75}Ni_{10.12}Al_{10}$ BMG might delay the onset of fracture and improve the plasticity of the alloy. It also can be found in Fig. 3 that the radial shear bands propagate to a smaller outward distance in the $Zr_{64.13}Cu_{15.75}Ni_{10.12}Al_{10}$ BMG. The ratio of radius of plastic deformation region (from the center of indents to the outmost shear band tip to the radius of the indent is 1.5 and 1.7 for $Zr_{64.13}Cu_{15.75}Ni_{10.12}Al_{10}$ and $Zr_{65}Cu_{15}Ni_{10}Al_{10}$ BMG, respectively. In this work, the indentation tests were carried out using the same load, and the $\sigma_{0.2}$ and E of the two BMG are comparable (Table 1). The larger spreading distance of the radial shear bands in the latter BMG indicates that the shear bands are easier to grow and propagate due to the larger shear strain is carried out by each single shear band. In contrast, the $Zr_{64.13}Cu_{15.75}Ni_{10.12}Al_{10}$ BMG with a relatively higher ν[5] tend to promote the nucleation of shear bands. This could be confirmed by a detailed observation of the shear band pattern (Fig. 3c), where shear band branching can be found as marked by the arrows.

The near-surface stress state for conical indentation is biaxial compression, wherein the radial compressive stress is significantly larger in magnitude than the tangential compressive stress[13]. Therefore the biaxial stress state is equivalent to uniaxial compression in the radial direction superposed with hydrostatic stress. The latter produces an angular invariant normal stress σ_n on shear planes, and therefore the slip line angle θ with respect to the radial loading direction should decrease ($\theta < 45°$) for pressure sensitive metallic glasses. The included angle between intersecting shear bands was measured (Fig. 3), and the shear plane angle $\theta = 44° \pm 1°$. This suggests that the two BMGs exhibit the pressure independent nature of the plastic deformation at the present indentation test condition.

During indentation, the indentation strain rate (ε_i) is a nonlinear function of time[18]. It is effectively infinite at the sample surface and decreases monotonically with time at higher depths. For the indentation experiments in our case, the maximum depth is about 98μm, consequently ε_i is about $5.1\times10^{-3}s^{-1}$. It is proposed that the effective strain rate (ε_e) is 0.071~0.286ε_i for a conical indenter[18]. Thus, average ε_e in our indentation test is in the order of $10^{-4}s^{-1}$. Thus, the strain rate during indentation is comparable to that of the uniaxial compressive test.

4. Conclusion

Plastic deformation features of $Zr_{64.13}Cu_{15.75}Ni_{10.12}Al_{10}$ and $Zr_{65}Cu_{15}Ni_{10}Al_{10}$ BMGs were studied by quasi-static compressive tests and depth sensitive macroindentation tests with a conical indenter. The former BMG exhibits significant macroscaled plasticity in contrast to the brittleness of the latter BMG. The investigation of the deformation regions around the indents reveals that radial and circular shear bands formed after indentation. $Zr_{64.13}Cu_{15.75}Ni_{10.12}Al_{10}$ BMG exhibits a higher number density of radial and 23% lower shear band spacing compared with those of $Zr_{65}Cu_{15}Ni_{10}Al_{10}$ BMG. Shear band branching and smaller plastic region are also observed in the ductile BMG.

Acknowledgments

The authors acknowledge the support by the National Natural Science Foundation of China (Grant Nos. 50571109, 10572142 and 10432050) and National Basic Research Program of China (973 Program, No. 2007CB613905).

References

1. W. L. Johnson, *MRS Bull* **24**, 42 (1999).
2. A. Inoue, *Acta Mater.* **48**, 279 (2000).
3. C. A. Schuh, T. C. Hufnagel and U. Ramamurty, *Acta Mater.* **55**, 4067 (2007).
4. F. Spaepen, *Acta. Metall.* **25**, 407 (1977).
5. Y. H. Liu, G. Wang, R. J. Wang, D. Q. Zhao, M. X. Pan, W. H. Wang, *Science* **315**, 1385 (2007).
6. A. Inoue, W. Zhang, T. Tsurui, A. R. Yavari, A. L. Greer, *Philos. Mag. Lett.* **85**, 221 (2005).
7. J. Das, M. B. Tang, K. B. Kim, R. Theissmann, F. Baier, W. H. Wang, J. Eckert, *Phys. Rev. Lett.* **94**, 205501 (2005).
8. Y. Zhang, W. H. Wang and A. L. Greer, *Nature Mater.* **5**, 857 (2006).
9. K. F. Yao, F. Ruan, Y. Q. Yang, N. Chen, *Appl. Phys. Lett.* **88**, 122106 (2006).
10. J. Schroers and W. L. Johnson, *Phys. Rev. Lett.* **93**, 255506 (2004).
11. U. Ramamurty, S. Jana, Y. Kawamura and K. Chattopadhyay, *Acta Mater.* **53**, 705 (2005).
12. C. G. Tang, Y. Li and K. Y. Zeng, *Mater. Sci. Eng. A* **384**, 215 (2004).
13. G. R. Trichy, R. O. Scattergood, C. C. Koch and K. L. Murty, *Scripta Mater.* **53**, 1461 (2005).
14. D. M. Xing, T. H. Zhang, W. H. Li and B. C. Wei, *J. Alloy Compd.* **433**, 318 (2007).
15. Y. Kawamura, T. Shibata, A. Inoue and T. Masumoto, *Appl. Phys. Lett.* **69**, 1208 (1996).
16. W. H. Li, B. C. Wei, T. H. Zhang, L. C. Zhang and Y. D. Dong, *Mater. Trans.* **12**, 2954 (2005).
17. R. D. Conner, Y. Li, W. D. Nix and W. L. Johnson, *Acta Mater.* **52**, 2429 (2004).
18. W. H. Poisl, W. C. Oliver and B. D. Fabes, *J. Mater. Res.* **10**, 2024 (1995).